Cell

Evolutionary Divergence of Enzymatic Mechanisms for Posttranslational Polyglycylation

Krzysztof Rogowski,[1] François Juge,[2] Juliette van Dijk,[1] Dorota Wloga,[3] Jean-Marc Strub,[4] Nicolette Levilliers,[5] Daniel Thomas,[6] Marie-Hélène Bré,[5] Alain Van Dorsselaer,[4] Jacek Gaertig,[3] and Carsten Janke[1,*]
[1]CRBM, CNRS, Université Montpellier 2 and 1
[2]IGMM, CNRS, Université Montpellier 2
Montpellier 34293, France
[3]Department of Cellular Biology, University of Georgia, Athens, GA 30602-2607, USA
[4]LSMBO, Université Louis Pasteur, CNRS, Strasbourg 67087, France
[5]Laboratoire de Biologie Cellulaire 4, CNRS, Université Paris-Sud 11, Orsay 91405, France
[6]Interactions Cellulaires et Moléculaires, CNRS, Université de Rennes 1, Rennes 35042, France
*Correspondence: carsten.janke@crbm.cnrs.fr
DOI 10.1016/j.cell.2009.05.020

SUMMARY

Polyglycylation is a posttranslational modification that generates glycine side chains on proteins. Here we identify a family of evolutionarily conserved glycine ligases that modify tubulin using different enzymatic mechanisms. In mammals, two distinct enzyme types catalyze the initiation and elongation steps of polyglycylation, whereas *Drosophila* glycylases are bifunctional. We further show that the human elongating glycylase has lost enzymatic activity due to two amino acid changes, suggesting that the functions of protein glycylation could be sufficiently fulfilled by monoglycylation. Depletion of a glycylase in *Drosophila* using RNA interference results in adult flies with strongly decreased total glycylation levels and male sterility associated with defects in sperm individualization and axonemal maintenance. A more severe RNAi depletion is lethal at early developmental stages, indicating that protein glycylation is essential. Together with the observation that multiple proteins are glycylated, our functional data point towards a general role of glycylation in protein functions.

INTRODUCTION

Polyglycylation is a posttranslational modification that generates side chains of glycine on the γ-carboxyl groups of specific glutamate residues of target proteins (Bré et al., 1998; Vinh et al., 1999). Similarly to polyglutamylation (Eddé et al., 1990), this posttranslational modification was discovered on tubulin, where it occurs within the carboxy-terminal tail domains (Redeker et al., 1994). While polyglutamylation was observed on many different types of microtubules (MTs), polyglycylation is particularly prominent in cilia and flagella and is mostly found in cells that possess these organelles (Bré et al., 1996; Levilliers et al., 1995).

Functional experiments on tubulin glycylation were difficult to perform since the modifying enzymes were unknown. Initial insights into the potential function of polyglycylation were obtained using modification-specific antibodies. For example, anti-glycylation antibodies affected axoneme beating in vitro, suggesting that tubulin polyglycylation could regulate ciliary dynein (Bré et al., 1996). In *Tetrahymena*, the elimination of the major glycylation sites on β-tubulin was lethal or led to severe axonemal defects, including short axoneme size, absence of the central pair MTs, and incomplete outer doublet MTs (Redeker et al., 2005; Thazhath et al., 2002; Xia et al., 2000). Thus, tubulin glycylation could be an important regulator of both the assembly and functions of axonemal MTs. The recent observations that non-tubulin proteins are also substrates of polyglycylation (Ikegami et al., 2008; Lalle et al., 2006; Xie et al., 2007) indicate that glycylation is a posttranslational modification of general importance.

Here we describe the discovery of a group of enzymes that catalyze tubulin glycylation and show that some of these enzymes have non-tubulin substrates. We demonstrate that glycylases are members of the tubulin tyrosine ligase-like (TTLL) family, which already contains three types of known amino acid ligases, the tubulin tyrosine ligase (TTL; Ersfeld et al., 1993), polyglutamylases (Janke et al., 2005; van Dijk et al., 2007; Wloga et al., 2008), and an enzyme that ligates glycine to nucleosome assembly protein 1 (NAP1; Ikegami et al., 2008). We show that in mouse, TTLL3 and TTLL8 proteins are initiating glycylases with different substrate specificities, whereas TTLL10 is the elongating polyglycylase. In mammals, cooperation of these two types of enzymes generates polyglycine side chains in mammals, whereas in *Drosophila*, bifunctional enzymes catalyze both reactions. We also demonstrate that the previously reported absence of long glycine side chains on human sperm tubulin (Bré et al., 1996) is caused by two inactivating amino acid substitutions in human TTLL10. Finally, we show by RNA

interference (RNAi) that depletion of one of the two glycylases in *Drosophila* leads to strong reduction in polyglycylation, which causes defects in sperm maturation and results in male sterility. Moreover, expression of interfering RNA under a stronger promoter is lethal in early developmental stages. This suggests that polyglycylation is important for whole organism development in *Drosophila*. The identification of additional substrates of glycylation indicates that this modification could have a broad range of functions.

RESULTS

Identification of Murine Glycylases

Our study was initiated with the hypothesis that tubulin glycylases, like two other types of tubulin amino acid ligases, TTL (Ersfeld et al., 1993) and polyglutamylases (Janke et al., 2005; van Dijk et al., 2007), are members of the TTLL protein family. Within the mammalian TTLL family, TTLL3, 8, 10, and 12 remained uncharacterized. According to phylogenetic studies, the *TTLL12* gene is present in species that appear to lack glycylation (Janke et al., 2005; Schneider et al., 1997), and murine TTLL12 has no glycylation activity in vivo and in vitro (K.R., unpublished data). In contrast, the presence of orthologs of *TTLL3*, *8*, and *10* in genomes of diverse species (Janke et al., 2005) correlates with the known presence of tubulin glycylation, and a recent study showed that one of these three genes, *TTLL10*, encodes a glycylase for NAPs (Ikegami et al., 2008).

To test whether mouse TTLL3, 8, and 10 have a tubulin glycylase activity, we expressed the respective cDNAs (van Dijk et al., 2007) in HEK293 cells and tested the cell extracts in an in vitro MT glycylation assay. To distinguish between two possible types of activities, initiation (addition of the first glycine to a γ-carboxyl group of the target glutamate residue) and elongation of glycine side chains, we used substrates differing in the levels of tubulin glycylation: MTs polymerized from brain tubulin (that lack detectable glycylation) and strongly glycylated MTs of ciliary axonemes of *Tetrahymena thermophila*. Both TTLL3 and 8 promoted incorporation of [^{3}H]-glycine into brain MTs but had very low activity on axonemal MTs. In contrast, TTLL10 was almost inactive on brain MTs but promoted efficient [^{3}H]-glycine incorporation into axonemal MTs (Figure 1A). These observations suggest that TTLL3 and 8 are initiating glycylases, whereas TTLL10 is an elongating glycylase (polyglycylase) for tubulin. A similar functional specialization has been previously observed among polyglutamylases (van Dijk et al., 2007; Wloga et al., 2008).

We also examined the selectivity of the enzymes for α- and β-tubulin. TTLL3 and 8 modified both α- and β-tubulin of brain MTs, with TTLL8 showing preference for α-tubulin (Figure 1A). For TTLL10, which modified only axonemal MTs, two-dimensional electrophoresis was used to separate axonemal α- and β-tubulin. Using anti-α- or β-tubulin antibodies as well as TAP952 (an antibody that recognizes monoglycylated sites on tubulins; Bré et al., 1998), we found that both tubulin subunits of *Tetrahymena* axonemes are monoglycylated and thus are potential substrates for the elongation reaction. However, TTLL10 incorporated [^{3}H]-glycine mainly into α-tubulin (Figure 1B).

Next, we expressed TTLL3, 8, and 10 in U2OS cells and labeled the cells with antibodies that are specific to either mono- or polyglycylation: TAP952 and polyG (polyG specifically recognizes polyglycine chains; Duan and Gorovsky, 2002), respectively (Figure 1C). Nontransfected U2OS cells show no reactivity with either of these two antibodies (arrowheads). After expression of TTLL3 or 8, we detected specific labeling of MTs with TAP952 but not with polyG. Thus, TTLL3 and 8 mediate initiation of glycine side chains on MTs in vivo but not side chain elongation. In contrast, cells expressing TTLL10 alone showed no labeling with TAP952 but had a diffuse labeling with polyG that did not correspond to MTs. This suggests that TTLL10 adds polyglycine chains directly onto proteins that are not associated with MTs, while it cannot modify MTs without prior monoglycylation.

Two-Step Glycylation Mechanism in Mammals

To test whether the two types of mammalian glycylases can function in a cooperative manner to create long side chains on MTs, we co-overexpressed either TTLL3 or 8 together with TTLL10 in U2OS cells. In both cases, we observed a strong labeling of MTs with the polyG antibody (Figure 2A). These results indicate that MTs have acquired polyglycine side chains, which was not the case when TTLL3, 8, or TTLL10 were expressed alone (Figure 1C).

On immunoblots, the monoglycylation-specific antibody TAP952 detected strong signals in the tubulin region upon expression of TTLL3 or 8 alone. Additional protein bands were labeled after TTLL8 expression, suggesting that TTLL8 can mediate glycylation of other non-tubulin proteins (Figure 2B). TTLL3 increased glycylation of mostly β-tubulin in U2OS cells, while it promoted modification of both α- and β-tubulin in the in vitro assay (Figures 2B and 1A). Thus, it appears that the substrate preferences of the glycylating enzymes change depending on additional factors. Neither TTLL3 nor TTLL8 alone generated polyG-reactive epitopes, indicating that they are indeed restricted to reactions that generate monoglycine side chains (Figure 2B). In contrast, no TAP952 labeling was detected in extracts of cells expressing TTLL10. However, a strong polyG signal was induced on two distinct protein bands, one of them the size of α-tubulin (Figure 2B). We demonstrate that the substrate in the tubulin region corresponds to NAPs. First, two-dimensional immunoblot analysis shows that the polyglycylated 50 kDa protein band superimposes with NAPs but not with tubulins (Figure 2C), and second, ectopically expressed NAP1-EYFP and NAP2-EYFP were strongly polyglycylated by TTLL10 (Figure S1 available online). This is in agreement with the results of Ikegami et al. (2008) and indicates that in contrast to tubulins, NAPs can be polyglycylated directly by TTLL10.

After coexpression of TTLL3 or 8 with TTLL10, no TAP952 labeling was detected, whereas several protein bands were labeled with the polyG antibody. Virtually all protein bands labeled with TAP952 after expression of TTLL3 or 8 alone became labeled with polyG when TTLL10 was coexpressed (Figure 2B), suggesting that following monoglycylation by TTLL3 or 8, TTLL10 elongates glycine side chains of all major substrates of the initiating enzymes. The efficiency of this process is illustrated by the reduction of monoglycylated epitopes below detectable levels. This further indicates that the substrate specificity of polyglycylation in mammals is predetermined by the specificity of the initiating

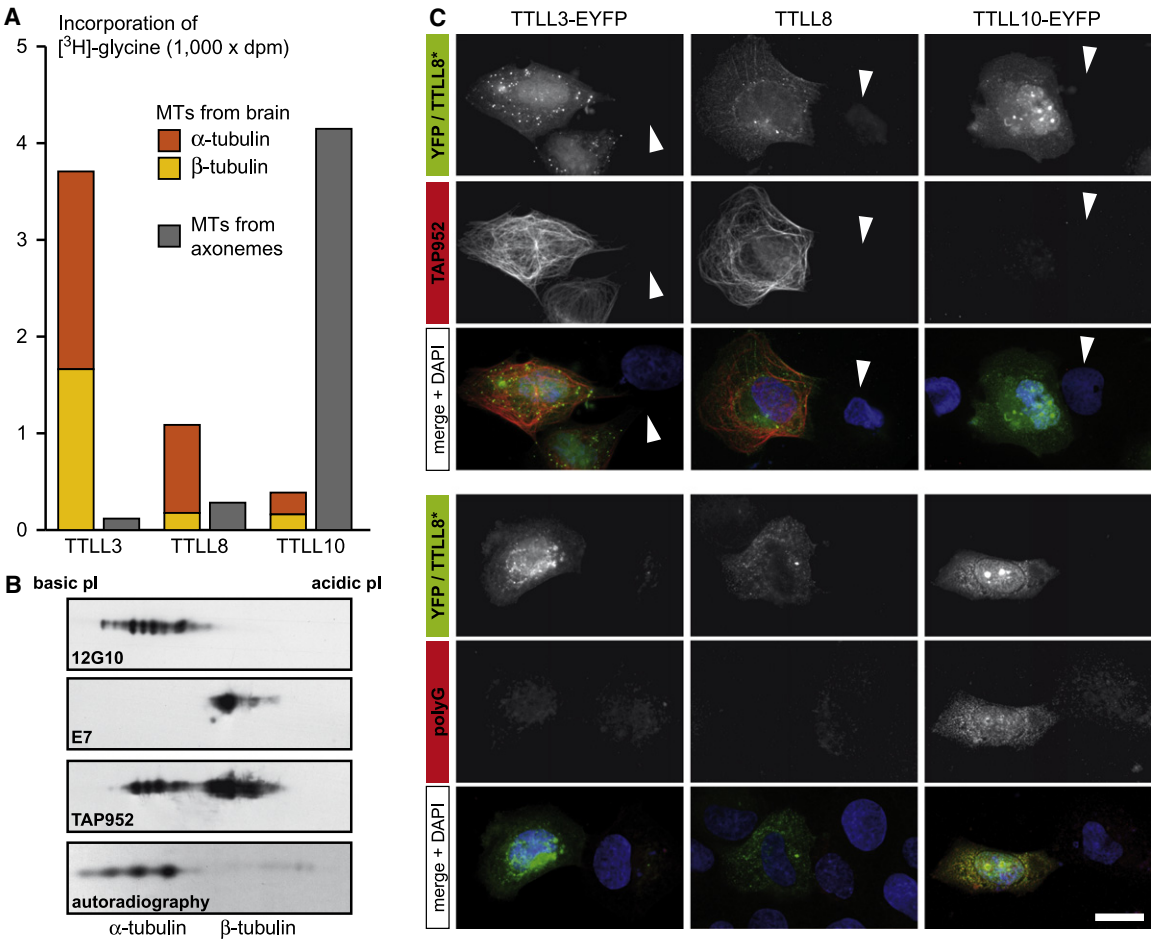

Figure 1. Enzymatic Characterization of Murine Glycylases

(A) In vitro glycylation activity of TTLL3, 8, and 10 using brain MTs that lack detectable glycylation and highly glycylated *Tetrahymena* axonemal MTs as substrates. The incorporation of [^{3}H]-glycine was separately determined for α- and β-tubulin for brain, but not for axonemal MTs due to comigration of both tubulin subunits.

(B) Two-dimensional analysis of α- and β-tubulin from *Tetrahymena* ciliary axonemes (12G10: anti-α-tubulin; E7: anti-β-tubulin). While both tubulin subunits are monoglycylated (TAP952 panel), the TTLL10-enriched fraction incorporates [^{3}H]-glycine mainly into α-tubulin in vitro (autoradiography panel).

(C) Immunofluorescence analysis of U2OS cells overexpressing TTLL3-EYFP, TTLL8, or TTLL10-EYFP. TAP952 labels the MT cytoskeleton of cells expressing TTLL3 or 8 but not TTLL10. PolyG antibody detects a diffuse staining after TTLL10 overexpression. Nontransfected cells, visualized by DAPI staining of the nuclei, are labeled with neither TAP952 nor polyG (arrowheads). *TTLL8 was expressed as an untagged protein and detected with anti-TTLL8 antibody. Scale bar is 20 μm.

glycylases rather than by the specificity of elongating enzymes, except for proteins that are directly modified by TTLL10, such as the NAPs.

Loss of Elongating Activity in Humans

Human sperm axonemes, unlike sperm axonemes of several other mammalian species studied so far, have side chains limited to monoglycylation (Bré et al., 1996). We confirmed this by comparing the status of glycylation in protein extracts prepared from mouse, rhesus monkey, and human sperm using the TAP952 and the polyG antibody (Figure 3A). Several mouse and rhesus protein bands were strongly labeled with polyG, while only weak signals were detected with TAP952. In contrast, human sperm proteins were not labeled with polyG but strongly with TAP952. No differences between the three species were found for the related tubulin modification, polyglutamylation (Figure 3A, panel polyE).

To determine the molecular basis for the lack of elongated polyglycine chains in human sperm, we investigated the only known elongating glycylase in mammals, TTLL10. First, we confirmed the presence of a full-length mRNA by cloning *TTLL10* from human testes cDNA. We then expressed human, mouse, and rhesus TTLL10 in U2OS cells. The mouse and rhesus TTLL10 generated polyglycylation that could be specifically detected with polyG, whereas the human protein was inactive (Figure 3B). Accordingly, when cell extracts from HEK293 cells overexpressing the respective TTLL10 proteins were used for in vitro assays, only the mouse and rhesus, but not the human, TTLL10 mediated incorporation of [^{3}H]-glycine into axonemal MTs (Figure 3C). Domain-swapping experiments localized the

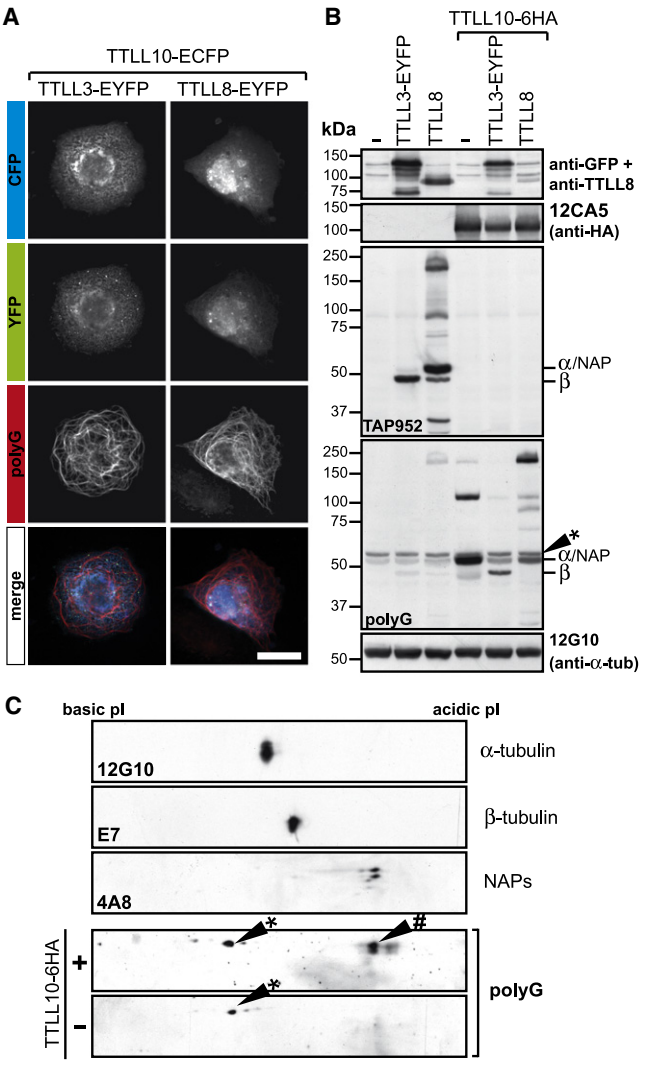

Figure 2. The Cooperative Mechanism of Murine Glycylases

(A) Immunofluorescence of U2OS cells coexpressing TTLL10-ECFP together with TTLL3-EYFP or TTLL8-EYFP. Note that polyG antibody labels the cytoskeleton. Scale bar is 20 μm.

(B) Immunoblot analysis of extracts from U2OS cells expressing TTLL3-EYFP, TTLL8, and TTLL10-6HA alone as well as TTLL3-EYFP or TTLL8 in combination with TTLL10-6HA. TAP952 recognizes protein bands exclusively in cell extracts after expression of TTLL3 or 8. Different proteins are detected with polyG antibody after overexpression of TTLL10 alone or in combination with TTLL3 or 8.

(C) Two-dimensional electrophoresis and immunoblot of extracts from control U2OS cells (–) or cells expressing TTLL10-6HA (+). The positions of α- and β-tubulin as well as NAPs are determined with specific antibodies. (# polyglycylated NAPs; * nonspecific polyG signal).

inactivating mutations to the central region of human TTLL10, which corresponds to the highly conserved core TTL domain (Figures S3, S4A, and S4B; van Dijk et al., 2007). Within this domain, human and rhesus TTLL10 differ by 11 amino acids, out of which 4 are not evolutionarily conserved. Thus, we analyzed the remaining 7 amino acid changes by introducing them separately into the rhesus TTLL10. Two of these mutations led to a complete loss of polyglycylase activity (Figures S3 and S4C), suggesting that the corresponding amino acids are essential for activity. When these two mutations in human TTLL10 were both reverted to the conserved amino acids found in rhesus and mouse, the enzyme recovered polyglycylase activity (Figures 3D and 3E). This was not the case if only one mutation was reverted. As neither of the two mutations has been found in the genomes of the great apes (not shown), it appears that humans are unique in having lost the polyglycylation activity of TTLL10. One of the two inactivating mutations (mut3) is polymorphic in the human population, leading to a high incidence (55.0% heterozygote and 16.7% homozygote) of *TTLL10* alleles without mut3 in the sub-Saharan African population, whereas 91.7% of the European population are homozygous for the presence of mut3 (http://www.ncbi.nlm.nih.gov/SNP/snp_ref.cgi?rs=1320571). No polymorphism was found for mut5. To investigate if the mut3 polymorphism could affect the enzymatic activity of TTLL10, we compared polyglycylation of sperm proteins from two homozygote individuals either with or without mut3 but both bearing mut5 (Figure S5A). The complete absence of polyglycylation on sperm proteins from both individuals (Figure S5B) confirmed that the presence of one of the two inactivating mutations is sufficient for the complete loss of enzymatic activity of human TTLL10 (Figure S4C).

In conclusion, we show that the human elongating glycylase TTLL10 is functionally inactive due to two mutations, resulting in the absence of polyglycylation in sperm. Considering that all known amino acid ligases that modify tubulin are members of the TTLL family, and that all TTLLs are expressed in testes (Ersfeld et al., 1993; van Dijk et al., 2007), it is likely that TTLL10 is the only polyglycylating enzyme in mammals. Thus, humans could be a unique mammalian species that lacks protein polyglycylation.

Cancer-Associated Mutations Inactivate the TTLL3 Enzyme

In a recently published screen for putative cancer-associated genes, *TTLL3* obtained a relatively high score as a potential cancer gene (Sjöblom et al., 2006). It was striking that the two mutations identified in the screen were localized in the vicinity of the ATP-binding residue E662, which is essential for enzymatic activity in all TTLLs (Figure 4A; van Dijk et al., 2007). To test the potential impact of these mutations, we introduced them separately into mouse TTLL3, which is identical to human TTLL3 in this region (Figure 4A), and tested the enzymatic activity of the mutated enzymes. Each cancer-related mutation led to a complete loss of glycylase activity of TTLL3 in vivo and in vitro (Figures 4B–4D), suggesting that reduction of monoglycylating activity could be related to cancer.

A Divergent Polyglycylation Mechanism in *Drosophila*

In mammals, TTLL10 appears to be the only enzyme able to elongate glycine side chains. However, in *Drosophila*, an organism with polyglycylated MTs (Bré et al., 1996), only two orthologs of the *TTLL3/8* group are present, whereas no *TTLL10* gene has been found (Janke et al., 2005). To establish the enzymatic mechanism that leads to the elongation of glycine side chains in the absence of TTLL10, we investigated the activity of the *Drosophila melanogaster* (dm) enzymes dmTTLL3A

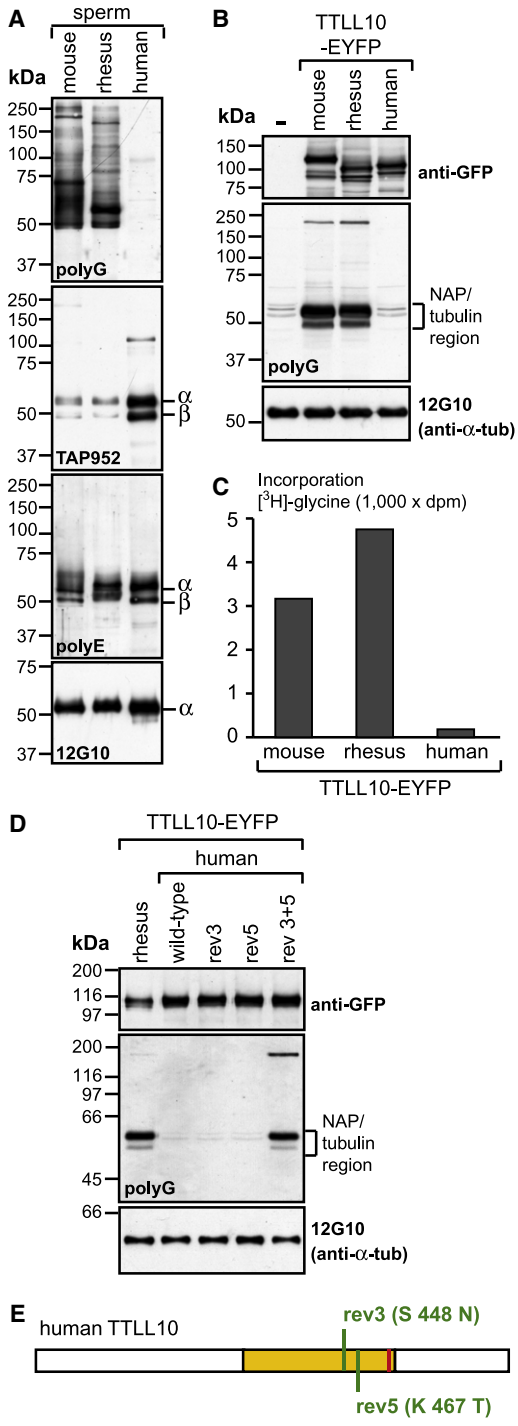

Figure 3. Evolutionary Loss of Polyglycylation in Humans

(A) Immunoblot analysis of mouse, rhesus, and human sperm proteins. The polyG antibody detects specific protein bands in mouse and rhesus, but not in human sperm. In contrast, TAP952 detects tubulin bands at a low level in mouse and rhesus but strongly in human. The polyE antibody labels tubulin of all three species equally strong.

(B) Immunoblot analysis of extracts from U2OS cells expressing mouse, rhesus, or human TTLL10.

(C) In vitro enzymatic assay of mouse, rhesus, and human TTLL10 expressed in HEK293 cells with axonemal MTs as a substrate.

(D) Immunoblot of U2OS cells expressing wild-type rhesus and human TTLL10, as well as human TTLL10 containing sequence reversions to amino acids present in rhesus and mouse TTLL10 (see Figure S3): S 448 N (rev3; reversion of mut3; see Figure S4C), K 467 T (rev5; reversion of mut5; see Figure S4C), or both of them (rev3+5). Wild-type rhesus TTLL10 and human TTLL10 carrying both rev3 and rev5 generated a strong polyG signal on NAPs, indicative of polyglycylase activity.

(E) Schematic representation of the human TTLL10 protein indicating the localization of the two amino acid reversions that allowed for reactivation of polyglycylase activity. The localization of the conserved core TTL domain (yellow) and the essential ATP-binding residue E511 are indicated (red; Figure S3; van Dijk et al., 2007).

(CG11323) and dmTTLL3B (CG11201) in U2OS cells. Both enzymes induced monoglycylation on MTs (Figure 5A, panel TAP952). Some cells expressing dmTTLL3B showed a restricted localization of this enzyme to the nucleus, and accordingly, only the nucleus was labeled with TAP952 in those cells (Figure 5A, #). However, in contrast to the mammalian orthologs (Figure 1C), dmTTLL3A also generated polyglycylated MTs as detected with polyG, while dmTTLL3B polyglycylated nuclear proteins but not MTs (Figure 5A, panel polyG). Immunoblots revealed that dmTTLL3A initiates and elongates glycine side chains on α- and β-tubulin, whereas dmTTLL3B initiates glycylation on a number of proteins including α-tubulin but functions as an elongating glycylase only for non-tubulin substrates (Figure 5B). These polyglycylated substrates of yet unknown identity are likely to be responsible for the observed nuclear staining (Figure 5A). Thus, *Drosophila* has a polyglycylation mechanism that utilizes bifunctional initiating/elongating glycylases.

dmTTLL3B Is Essential in *Drosophila*

Polyglycylation is particularly abundant in testes where it is associated with the axonemes of the sperm flagella (Bré et al., 1996; Bressac et al., 1995). In *Drosophila*, one of the polyglycylase genes, *dmTTLL3B*, is highly expressed in testes (Figure S6), suggesting that dmTTLL3B is the major polyglycylase in this organ. Thus, we attempted to deplete dmTTLL3B by RNAi, using a transgenic fly carrying inverted repeats that correspond to *dmTTLL3B* under the control of *UAS* sequences inducible by *Gal4* (*UAS-IR-dmTTLL3B* transgene). Strikingly, 50% of the embryos carrying *UAS-IR-dmTTLL3B* and the ubiquitous *da-Gal4* driver ($dmTTLL3B^{da\text{-}RNAi}$) did not survive to adulthood (Figure 6A).

RT-PCR analysis of adult $dmTTLL3B^{da\text{-}RNAi}$ flies demonstrated that *dmTTLL3B* inverted repeats were expressed and *dmTTLL3B* mRNA levels were strongly decreased. In contrast, mRNA levels of the closest homolog of this gene, *dmTTLL3A*, were unchanged (Figure 6B), demonstrating the specificity of the *dmTTLL3B* RNAi. Immunoblots of whole-protein extracts showed a strong reduction of polyG labeling on a range of protein bands in the $dmTTLL3B^{da\text{-}RNAi}$ flies (Figure 6C), whereas polyglutamylation levels were slightly increased in males but not in females (Figure 6C, panel GT335). These data provide strong evidence that the majority of the protein polyglycylation in *Drosophila* is catalyzed by dmTTLL3B. Almost all adult male $dmTTLL3B^{da\text{-}RNAi}$ flies were sterile, as only 2.4% were able to generate offspring (Figure 6D), although with 20 times less progeny as compared to wild-type. This suggests that polyglycylation is important for spermatogenesis.

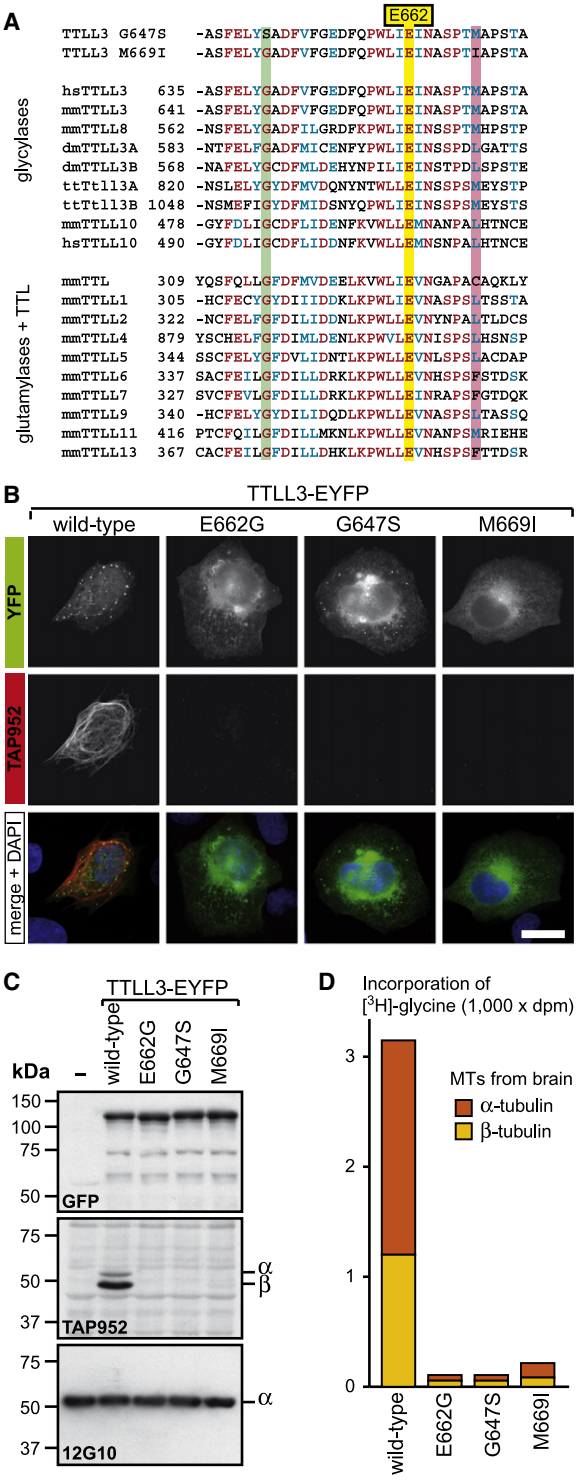

Figure 4. Loss of Enzymatic Activity of TTLL3 in Colon Cancer

(A) Sequence alignment of different TTLL proteins from different organisms maps the position of two cancer-related mutations in TTLL3 (G647S: green, M669I: pink; Sjöblom et al., 2006) to two highly conserved residues in the vicinity of the conserved ATP-binding site (E662: yellow). Amino acids in red letters: identity; in blue: similarity.

(B) TAP952 labeling of U2OS cells expressing wild-type TTLL3-EYFP and the mutated proteins including the E662G ATPase dead version. Scale bar is 20 μm.

(C) Immunoblot of extracts from U2OS cells expressing wild-type and mutated TTLL3s.

(D) In vitro glycylation assay of extracts from HEK293 cells expressing either the wild-type or mutated forms of TTLL3, using brain MTs as substrate.

The process of spermatogenesis in *Drosophila* can be divided into three major steps: (1) the generation of 64 haploid, interconnected spermatocytes from a stem cell, (2) the formation of the axonemes and the condensation of the sperm nuclei in the still interconnected spermatids, and (3) the individualization that resolves the syncytial sperm bundle into 64 separate sperm cells. This last step is achieved by a group of synchronously moving individualization complexes that remove excess cytoplasm and place the membranes around each cell. To determine which of the three steps were affected in *dmTTLL3B*$^{da\text{-}RNAi}$ flies, we analyzed the testes by immunofluorescence and transmission electron microscopy (TEM). In immunofluorescence (Figure 6E) of wild-type testes, the polyG antibody stained prominent bundles of fibers that correspond to the sperm tails. The actin staining visualized groups of regularly arranged individualization complexes, which were always associated with the polyG-reactive MT bundles, confirming that sperm polyglycylation appears at the onset of individualization (Bré et al., 1996; Bressac et al., 1995). In contrast, in *dmTTLL3B*$^{da\text{-}RNAi}$ testes, polyG staining was strongly reduced and actin cones were scattered along the tails, indicating a sperm individualization defect (Fabrizio et al., 1998). Moreover, we observe that the tips of the testes were often enlarged in *dmTTLL3B*$^{da\text{-}RNAi}$ male flies (Figure 6E).

To better understand the observed defects, we used TEM to compare cross-sections of sperm cysts at different stages of maturity. In the preindividualization stage, sperm cysts of both control and *dmTTLL3B*$^{da\text{-}RNAi}$ flies appeared similar, as they contained the expected 64 sperm cells with an axoneme as well as a minor and a major mitochondrial derivate (Figure 6F). Upon maturation, sperm cysts become more compact due to strongly reduced cytoplasmic ground substance. At this late stage, control cysts were highly organized as each axoneme was positioned in the close proximity of a major mitochondrial derivate (Figure 6G, panel control). In contrast, most of the mature cysts from *dmTTLL3B*$^{da\text{-}RNAi}$ flies were lacking the axoneme structures, whereas the mitochondrial derivates were still present (Figure 6G, panels *dmTTLL3B*$^{da\text{-}RNAi}$). In some cases, disorganized axonemes composed of singlet MTs were found. We also observed rare cases of disorganized cysts that still contained axonemes but had reduced or absent mitochondria. Together our findings indicate that polyglycylation plays a role in individualization and is essential for the maintenance of the axoneme structure at later stages. However, it is not required for the early steps of *Drosophila* spermatogenesis, including the assembly of the axonemes.

Finally, we hypothesized that the initially observed partial lethality of the *dmTTLL3B*$^{da\text{-}RNAi}$ flies indicates an essential function of *dmTTLL3B* in *Drosophila*, and that the flies that reached adulthood survived due to the incomplete suppression of *dmTTLL3B* under the *da-Gal4* driver. To test this hypothesis, we increased the efficiency of the RNAi by introducing the *UAS-Dcr-2*

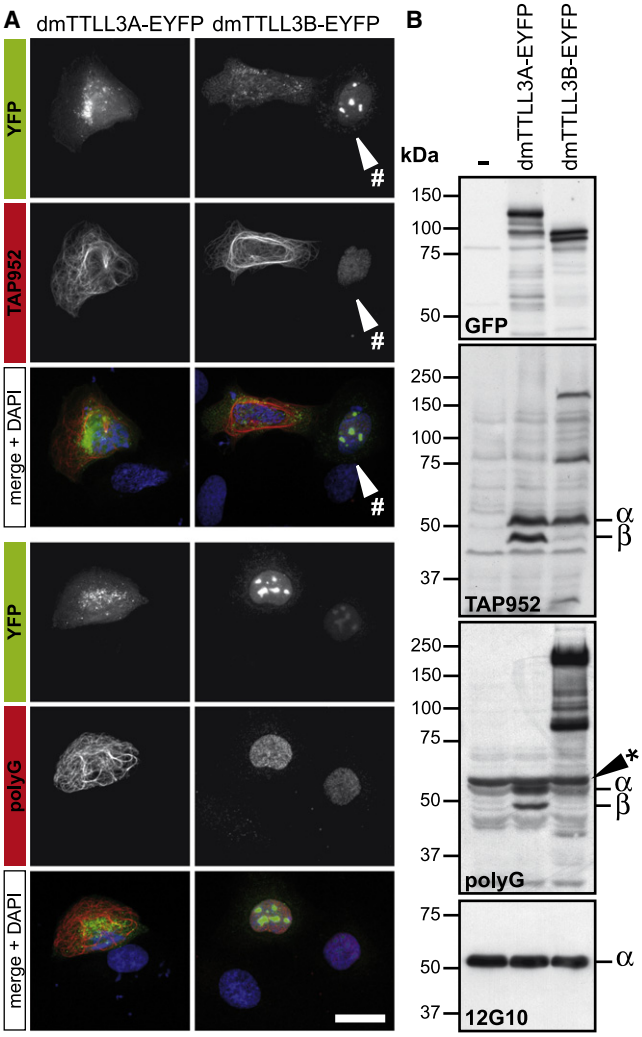

Figure 5. The Enzymatic Mechanism of Polyglycylation in *Drosophila*

(A) Immunofluorescence analysis of U2OS cells expressing *Drosophila melanogaster* (dm) TTLL3A-EYFP and TTLL3B-EYFP proteins. TAP952 labels cytoskeletal structures in cells expressing either of these proteins; however, some cells with a dominant nuclear localization of dmTTLL3B (#) show only diffuse nuclear labeling with this antibody. PolyG decorates the cytoskeleton in cells expressing dmTTLL3A but only the nucleus in the cells that express dmTTLL3B. Nontransfected cells are visualized by DAPI staining of the nuclei. Scale bar is 20 μm.

(B) Immunoblot analysis of extracts from U2OS cells expressing dmTTLL3A and dmTTLL3B. Both enzymes generate specific labeling of protein bands with the TAP952 and polyG antibodies. (* nonspecific polyG signal)

transgene (Dietzl et al., 2007) into the *dmTTLL3B*$^{da\text{-}RNAi}$ flies. Strikingly, we observed 100% lethality at the larval stage. This phenotype is not due to side effects of the *UAS-Dcr-2* transgene (Dietzl et al., 2007) since the expression of *UAS-IR-dmTTLL3B* under the control of the very strong and ubiquitous *Act5C-Gal4* driver also led to 100% lethality (not shown). Thus, in addition to an important role in spermatogenesis, dmTTLL3B-mediated polyglycylation could be essential for *Drosophila* development.

Identification of Candidate Substrates of Glycylation

The observation that mouse TTLL8 as well as *Drosophila* TTLL3B glycylate a range of non-tubulin proteins (Figures 2B, 5B, and 6C) raised the possibility that glycylation is a posttranslational modification with a broad range of substrates. Following the observation that the two most prominent substrates of polyglutamylation, tubulins (Eddé et al., 1990) and NAPs (Regnard et al., 2000), are also modified by polyglycylation (Redeker et al., 1994; Ikegami et al., 2008), we hypothesized that additional substrates of glycylation are among the previously identified substrates of polyglutamylation (van Dijk et al., 2008). We expressed 12 potential substrates of polyglutamylation together with either TTLL8 or an enzymatically inactive (dead) version of TTLL8 in HEK293 cells. Five proteins (ANP32A, ANP32B, SET, RanGAP, and nucleolin) were found to be glycylated in the presence of active but not inactive TTLL8 (Figure 7). Seven other proteins tested (NF45, B23, GRP78, NASP, RNP-K, NCT, EB1; data not shown) were not modified. To uncover additional substrates by a more direct approach, we separated proteins from fly testes using two-dimensional electrophoresis and analyzed polyG-reactive proteins by mass spectrometry. We selected six of the identified proteins (Table S1; see Supplemental Data for more details) and co-overexpressed them with active or inactive TTLL8 in HEK293 cells. Among these proteins, troponin T was found to be specifically glycylated by ectopic TTLL8 (Figure 7). The identification of a range of potential substrates of glycylation suggests that this modification could regulate the function of many proteins. Thus, the lack of glycylation of several proteins, and not only tubulin, could have contributed to the defects observed in the dmTTLL3B-depleted flies.

DISCUSSION

Polyglycylation was first described as a polymodification that generates glycine side chains of variable lengths on α- and β-tubulins (Redeker et al., 1994). Similarly to polyglutamylation, it targets the C-terminal tails of tubulins, which are the major interaction sites for MT-associated proteins and molecular motors (Nogales, 2000). Thus, polyglycylation could be an important regulator of MT functions.

We have identified a group of enzymes that mediate the generation of glycine side chains on proteins. The glycylating enzymes are members of the TTLL family, which also contains other enzymes that catalyze amino acid ligations: tubulin tyrosine ligase (Ersfeld et al., 1993) and diverse polyglutamylases (Janke et al., 2005; van Dijk et al., 2007; Wloga et al., 2008). Initiation and elongation of the glycine side chains are catalyzed by separate glycylases in mammals. Two initiating enzymes, TTLL3 and TTLL8, both generate monoglycylation on tubulin, whereas only TTLL8 modifies additional proteins. In agreement with our results, TTLL3 proteins in the ciliate *Tetrahymena* and in zebrafish are also initiating tubulin glycylases (Wloga et al., 2009). The subsequent elongation of glycine side chains in mammals is catalyzed by the elongating glycylase TTLL10.

The discovery of a strict two-step mechanism for MT polyglycylation in vertebrates raised two questions related to previous descriptions of polyglycylation patterns in different organisms.

First, elongated glycine side chains are completely absent in human sperm tubulin (Bré et al., 1996). We show that this phenotype is directly related to human TTLL10, which lacks enzymatic activity due to two point mutations in the conserved core TTL domain. It is striking that these mutations appear to be unique to human TTLL10, which suggests that the loss of polyglycylation was an event important for human evolution. Furthermore, the existence of a species devoid of polyglycylation suggests that the "poly" character of glycylation is not essential for protein functions, and that the functions of glycylation could be efficiently fulfilled by monoglycylation, which is present in all cilia in mammals (Dossou et al., 2007). Another surprising observation was that *Drosophila*, an organism with reported polyglycine side chains on tubulin (Bré et al., 1996), has no homologs of *TTLL10*. We show that in *Drosophila*, glycylases from the TTLL3/8 group act as bifunctional enzymes that are able to catalyze both initiation and elongation of glycine side chains, explaining why polyglycine side chains are present despite the absence of a TTLL10 ortholog. The two distinct glycylation mechanisms in mammals and *Drosophila* correlate with the previously described order of appearance of polyglycylation during sperm maturation. In mouse, polyglycine side chain elongation is delayed, appearing only after initial monoglycylation (Kann et al., 1998), whereas in *Drosophila*, mono- and polyglycylation occur simultaneously (Bré et al., 1996).

In *Drosophila* the depletion of *dmTTLL3B* induced a significant decrease in glycylation, accompanied by decreased viability and an almost complete sterility of the surviving males. Detailed analysis of the *dmTTLL3B*$^{da\text{-}RNAi}$ flies revealed that the lack of dmTTLL3B affects late stages of spermatogenesis. This coincides with the timing of appearance of glycylation in *Drosophila* sperm development (Bressac et al., 1995). We observed that although axonemes assemble, they become unstable and disassemble in the final stages of spermatogenesis. The disassembly of the axonemes is likely to proceed through a stage in which MT doublets are reduced to singlets, followed by the complete disappearance of all MT structures. Thus, one of the roles of glycylation in spermatogenesis appears to be the maintenance of the axonemal structure, whereas the modification is not required for the assembly.

Due to their sensory role in cells, cilia are centers of signal transduction pathways involved in embryonic development and tissue homeostasis in adults. Therefore, defects in cilia can be related to cancer (Mans et al., 2008; Michaud and Yoder, 2006). Our finding that two cancer-related mutations in TTLL3 (identified by Sjöblom et al., 2006) both completely inactivate this enzyme suggests that the lack of TTLL3 activity could affect cilia, which in turn could contribute to cancer progression.

The complexity of signals generated by polyglutamylation and polyglycylation on MTs could allow for different modes of regulation. Besides the possibility that both polymodifications generate signals for different target proteins, glycylation could also function as a counter-regulator of polyglutamylation, since both modifications compete for similar modification sites on tubulin (Redeker et al., 2005). In agreement with this hypothesis, we show that tubulin polyglutamylation increases upon depletion of polyglycylation. Such a function could be sufficiently fulfilled by monoglycylation, which would help to explain the apparent lack of phenotypes related to the loss of elongated glycine side chains in humans.

Most of the past work on glycylation has been focused on the role of this modification in MT functions; however, several recent studies have shown that other proteins are substrates of glycylation (Ikegami et al., 2008; Lalle et al., 2006; Xie et al., 2007). Together with our results, this opens the possibility that glycylation targets a broad range of substrates.

To conclude, we have identified a group of tubulin-modifying enzymes and two evolutionarily divergent mechanisms for glycine side chain initiation and elongation. Functional studies in *Drosophila* show that glycylation is important for sperm maturation, and that it might also be essential in early developmental stages in flies. Finally, the discovery that several important proteins could undergo glycylation raises the possibility that this modification acts as a general regulator of cellular functions.

EXPERIMENTAL PROCEDURES

Cloning and Mutagenesis

Mouse *TTLL3*, *8*, and *10* have been identified and cloned before (van Dijk et al., 2007). The rhesus monkey (*Macaca mulatta*) *TTLL10* cDNA sequence was reconstructed from fragments found by NCBI Blast (http://blast.ncbi.nlm.nih.gov/) using known *TTLL10* sequences as templates. The predicted sequence was amplified from testis cDNA (BioChain Institute Inc., USA) and cloned, and the DNA was sequenced. PCR-related mutations were excluded by sequencing of multiple clones (complete coding sequence: Figure S2A). For human *TTLL10*, a splice variant (Figure S2C) of the sequence AK124125 has been amplified from testis cDNA (BioChain Institute Inc.) and verified by DNA sequencing. *Drosophila dmTTLL3A* (CG11323) and *dmTTLL3B* (CG11201) were cloned from cDNA from adult flies.

Point mutations were introduced by a PCR-based quick-change method. The presence of the mutation was verified by DNA sequencing.

Drosophila Genetics

Drosophila was grown on standard medium at 25°C. The w^{1118}, *UAS-IR-TTLL3B* transgenic line was obtained from the Vienna *Drosophila* RNAi Center (http://www.vdrc.at). The transgene, localized on the X chromosome, expresses an inverted repeat from the *dmTTLL3B* gene (*CG11201*) under the control of *UAS* sequences. *UAS-IR-TTLL3B* flies were crossed with strains carrying the *da-Gal4* (*dmTTLL3B*$^{da\text{-}RNAi}$) or the *Act5C-Gal4* driver. For amplification of the RNAi effect, the *da-Gal4* transgene was associated with the *UAS-Dcr-2* transgene (Dietzl et al., 2007), and the resulting strain was crossed with *UAS-IR-TTLL3B* flies. For the viability test, 352 control (*UAS-IR-TTLL3B*) and 510 *dmTTLL3B*$^{da\text{-}RNAi}$ embryos were scored for survival to adulthood (results represented in Figure 6A). Total RNA was extracted from adult flies with TRIZOL reagent (Sigma, USA), and reverse transcription was performed using the First-Strand cDNA synthesis kit (GE Healthcare, USA) with 5 μg of RNA and random hexamers as primers. 1/60 of this cDNA was used for PCR amplification. Primer pairs used for the detection of different gene transcripts can be provided on request. Number of PCR cycles used for RT-PCR: RNAi, dmTTLL3B: 30, dmTTLL3A: 35, rp49: 25. Male fertility was tested in individual crosses with w^{1118} females, and the presence of progeny was scored after 2 weeks. Fifty-five individual crosses were scored for control (*UAS-IR-TTLL3B*) and 83 for *dmTTLL3B*$^{da\text{-}RNAi}$ males (results represented in Figure 6D).

Isolation of Axonemes from *Tetrahymena* Cilia

CU427 *Tetrahymena* cells were grown in SPP medium (1% proteose peptone, 0.2% glucose, 0.1% yeast extract, 0.003% EDTA ferric sodium salt) at 30°C to mid-log phase (4–5 × 10^5 cells/ml). Cilia were collected as described (Brown et al., 1999) and stored at −80°C. For the preparation of axonemes, cilia were demembranated using 0.2% NP-40 in 1× ERB buffer (50 mM Tris/HCl, pH 8.0, 10% glycerol, 5 mM $MgCl_2$, 1 mM EGTA). To remove the endogenous glycylase

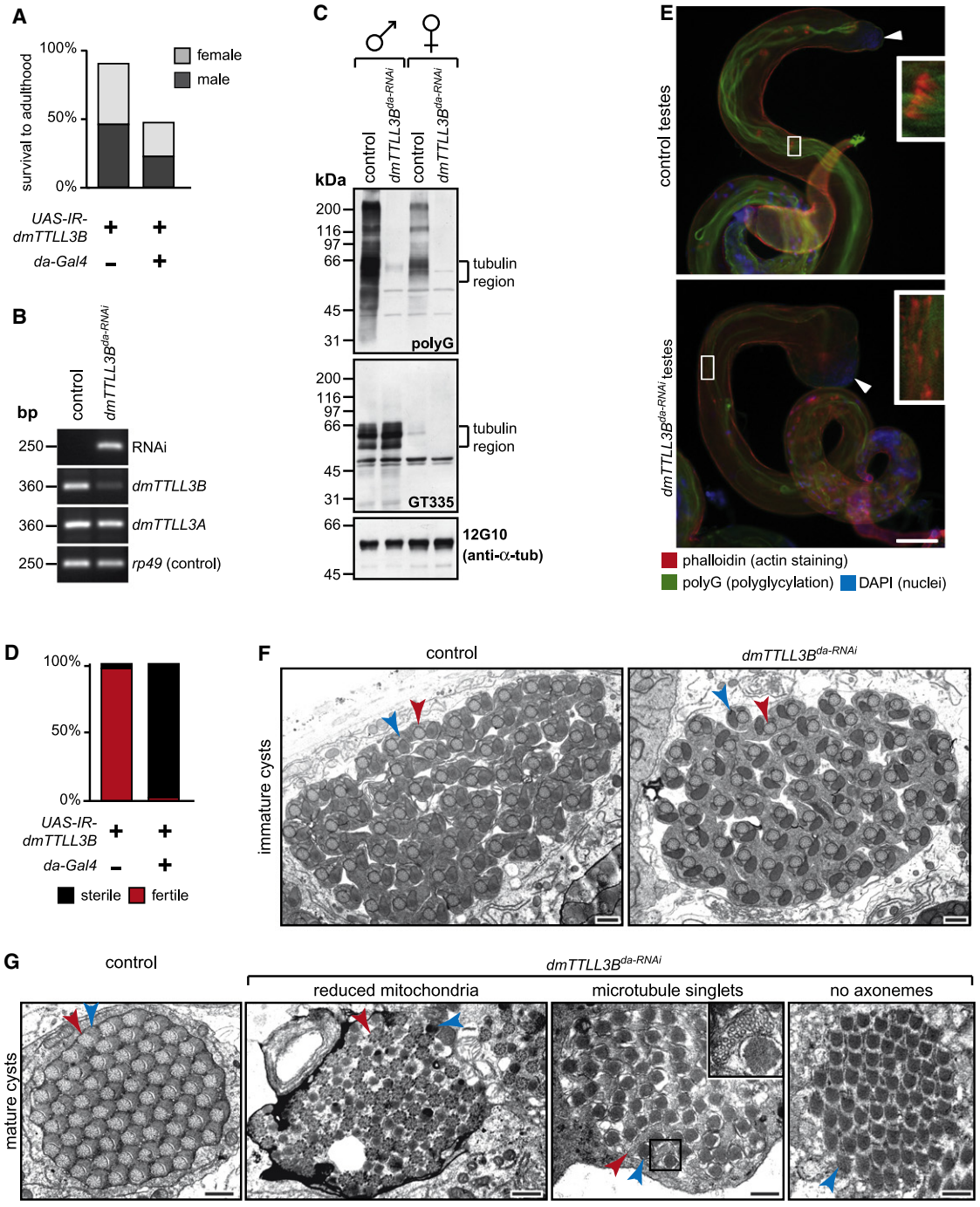

Figure 6. Effects of dmTTLL3B Depletion in *Drosophila*

(A) Comparison of the survival of female and male flies carrying *UAS-IR-dmTTLL3B* transgene in the presence or absence of the driver. The percentage of viable adult flies as compared to the number of embryos is shown.

(B) RT-PCR analysis of *dmTTLL3B*-RNAi, *dmTTLL3B*, *dmTTLL3A*, and *rp49* expression in control (*da-Gal4*/+) and *dmTTLL3B*$^{da\text{-}RNAi}$ flies.

(C) Immunoblots of whole-fly extracts, probed for polyglycylation (polyG), polyglutamylation (GT335), and α-tubulin (12G10). In control (*da-Gal4*/+) flies, multiple proteins are labeled with polyG antibody in male and female flies. This labeling is strongly reduced in *dmTTLL3B*$^{da\text{-}RNAi}$ flies. In contrast, polyglutamylation is only detected in male individuals and increases upon depletion of polyglycylation.

(D) Sterility of male flies carrying *UAS-IR-dmTTLL3B* transgene in the presence or absence of the driver.

(E) Immunofluorescence of testes from control (*da-Gal4*/+) and *dmTTLL3B*$^{da\text{-}RNAi}$ flies. Actin is stained with TRITC-conjugated phalloidin (red), and polyglycylated proteins are revealed with polyG antibody (green). Nuclei are stained with DAPI (blue). In *dmTTLL3B*$^{da\text{-}RNAi}$ flies, polyglycylation levels are decreased and actin cones are scattered. The tip of the testes (arrowhead) is enlarged. Insets show the distribution of actin cones (zoom 2.5×). Scale bar is 100 μm.

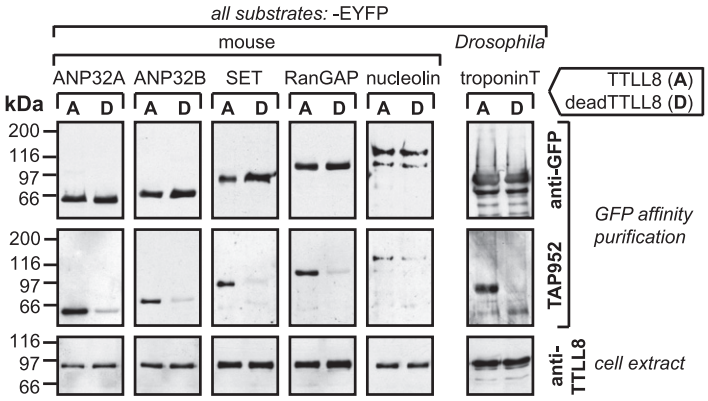

Figure 7. Substrates of Glycylation

EYFP-tagged mouse or *Drosophila* proteins were coexpressed with active (A) or inactive ("dead"; D) mouse TTLL8 in HEK293 cells. After EYFP affinity purification, proteins were detected with anti-GFP antibody, and the level of glycylation was determined with TAP952. The total extract was probed for TTLL8 expression with anti-TTLL8 antibody.

activity, axonemes were further treated with 1 M NaCl in 1× ERB for 30 min, followed by an incubation at 60°C for 20 min. Axonemes were spun down (12,000 g, 30 min, 4°C), and the supernatant was discarded. The pellet was then washed in 1× ERB and resuspended in 1× ERB at a final concentration of 5 mg/ml.

Tubulin Polyglycylation Assay

The enzymatic activity of glycylase was determined based on incorporation of [^{3}H]-glycine into MTs. The assay was performed in 50 μl of 1× ERB supplemented with 2 mM ATP and 250 pmol (5 μl) [^{3}H]-glycine (20.0 Ci/mmol; GE Healthcare). Enzymatic activity was measured using cell extracts prepared in 1× ERB containing 0.2% NP-40. Twenty micrograms of axonemal or taxotere-stabilized MTs (prepared from adult mouse brains as described; Regnard et al., 1999) were resuspended in the reaction mixture and immediately transferred to 30°C, followed by 4 hr of incubation. The samples were then subjected to SDS-PAGE (10% gels) and electrotransferred onto nitrocellulose membrane. The tubulin bands were visualized by staining with Ponceau S, cut out, and placed in 5 ml of scintillation liquid (Ultima Gold, Perkin Elmer, USA) for quantification. Alternatively, SDS-PAGE gels were stained with Coomassie blue and incubated in Amersham Amplify (GE Healthcare), and [^{3}H]-glycine incorporation was visualized by autoradiography. Absolute values can vary between enzymatic tests. Values shown in Figures 1A, 3C, and 4D are representative for multiple experiments.

Affinity Purification of EYFP-Tagged Proteins

EYFP-tagged potential substrates were coexpressed with TTLL8 in HEK293 cells. After lyses of the cells in PBS, 0.2% NP-40, the supernatant (100,000 g, 30 min, 4°C) was incubated with GFP-TRAP agarose beads (ChromoTek, Germany) for 4 hr at 4°C. Beads were washed twice in PBS, 0.2% NP-40 and boiled in Laemmli sample buffer for 5 min. The samples were spun at 20,000 g for 5 min and supernatants were analyzed by SDS-PAGE and immunoblot.

Protein Electrophoresis and Immunoblot

One-dimensional SDS-PAGE was performed using standard protocols, or a special protocol for the separation of mammalian α- and β-tubulin (Eddé et al., 1987). Two-dimensional electrophoresis consisted of an isolelectric focusing step (IPGphor Isoelectric Focusing System; GE Healthcare) and an SDS-PAGE. For the resolution of the tubulin in Figure 1B, 40 μg of tubulin were loaded on 18 cm pH 4.5–5.5 Immobiline strips (GE Healthcare). Cell extracts shown in Figure 2C were prepared directly in the loading buffer (7 M urea, 2 M thiourea, 4% [w/v] CHAPS, 2% [v/v] IPG buffer [GE Healthcare], 40 mM DTT) and resolved in 8.5 cm pH 3.0–5.6 Immobiline strips (GE Healthcare).

Membranes were incubated with the following antibodies: polyG (1:6000), polyE (1:1000; both courtesy of M. Gorovsky), TAP952 (Bré et al., 1998; ascitic fluid, 1:2000), 12G10 (Thazhath et al., 2002; 1:250), E7 (Chu and Klymkowsky, 1989; 1:20), 12CA5 (1:10), anti-GFP (1:5000; Torrey Pines Biolabs, USA), anti-NAP 4A8 (Fujii-Nakata et al., 1992; Ishimi et al., 1985; 1:20). Antibodies against TTLL8 were raised in rabbits with bacterially expressed protein and then purified on recombinant TTLL8 and used at 1:500 dilution.

Protein bands were visualized with HRP-labeled donkey anti-rabbit or anti-mouse IgG 1:10,000 (GE Healthcare) followed by detection with ECL immunoblot detection kit (GE Healthcare).

Immunofluorescence and Microscopy

U2OS cells were cultured on glass coverslips under standard conditions and fixed using a protocol for preservation of cytoskeletal structures (Bell and Safiejko-Mroczka, 1995). Fixed cells were incubated with TAP952 (hybridoma supernatant 1:200), polyG (1:3000), anti-TTLL8 (1:1000), or anti-GST (1:1000) antibody for 1 hr, followed by 30 min with anti-mouse or anti-rabbit Alexa 555 or Alexa 488 antibody (1:1000; Molecular Probes, USA). DNA was visualized by DAPI staining (0.02 μg/ml). Coverslips were mounted with MOWIOL. *Drosophila* testes were fixed for 30 min with 3.7% paraformaldehyde in PBS, permeabilized in PBS containing 0.5% Triton X-100, and incubated with polyG (1:9000) for 1 hr, followed by 30 min with anti-rabbit Alexa 647. Actin was visualized with TRITC-conjugated phalloidin (1:10,000; Sigma). We used DMRA microscopes (Leica, Germany) and Metamorph (Universal Imaging Corp., USA) software.

For ultrastructural analysis, testes were isolated from 3- to 4-day-old male flies and fixed in 3.5% glutaraldehyde in 100 mM phosphate buffer (pH 7.4) overnight at 4°C. The samples were rinsed in phosphate buffer and post-fixed in 1% osmic and 0.8% potassium ferrocyanide for 2 hr in the dark at room temperature (RT). After rinsing in phosphate buffer, samples were dehydrated in a series of ethanol solutions (30%–100%) and embedded in EmBed 812 DER 736. Eighty-five nanometer sections were cut on a Leica-Reichert Ultracut E microtome and counterstained with uranyl acetate and lead citrate. Images were acquired with a Hitachi 7100 transmission electron microscope at the Centre de Ressources en Imagerie Cellulaire de Montpellier (France).

ACCESSION NUMBERS

The *Macaca mulatta* TTLL10 sequence reported in this paper has been deposited in GenBank with accession number FN391584.

SUPPLEMENTAL DATA

Supplemental Data include six figures, Supplemental Experimental Procedures, and two tables and can be found with this article online at http://www.cell.com/supplemental/S0092-8674(09)00577-7.

ACKNOWLEDGMENTS

This work was supported by the CNRS; the Universities Montpellier 2 and 1; the Association pour la Recherche sur le Cancer (ARC) awards CR504/7817

(F and G) Transmission electron micrographs of sections of cysts from control (*da-Gal4*/+) and *dmTTLL3B*$^{da\text{-}RNAi}$ flies. Red arrowheads show axonemes, blue mitochondria. Scale bar is 500 nm. (F) Immature cysts of *dmTTLL3B*$^{da\text{-}RNAi}$ flies show no phenotypic abnormalities as compared to control. (G) Phenotype of mature cysts in control and *dmTTLL3B*$^{da\text{-}RNAi}$ flies. Abnormalities found in *dmTTLL3B*$^{da\text{-}RNAi}$ flies include reduced number of mitochondria, disorganized axoneme structures (singlet microtubules; inset with 2.5× zoom), and complete absence of axonemes.

and 3140 (to C.J.) and 4894 (to F.J.); the French National Research Agency (ANR) awards 05-JCJC-0035 and 08-JCJC-0007 to C.J.; and the Ligue contre le Cancer fellowship JG/VP-5454, the EMBO long-term fellowship ALTF 546-2006 to K.R. and NSF grant MBC-033965 to J.G. We thank J.-M. Donnay, G. Herrada-Aldrian, B. Lacroix, L. Linarès, J.-C. Mazur, J. Miro, D. Moustapha Abba Moussa, Y. Thomas (CRBM, Montpellier, France), V. Bäcker, J. Cau, S. DeRossi, P. Travo (RIO Imaging facility at the CRBM), and U. Rothbauer (ChromoTek GmbH, Martinsried, Germany) for technical assistance and C. Cazevieille (CRIC, Montpellier, France) for technical assistance and helping us to interpret the ultrastructural data. We are grateful to M. Bosch-Grau, A. Burgess, B. Eddé, B. Lacroix, M.M. Magiera, J. Miro, A.C. Seixas (CRBM), M. Bettencourt-Dias (Instituto Gulbenkian de Ciência, Oeiras, Portugal), M. Knop, I. Mattaj (EMBL, Heidelberg, Germany), and C. Sardet (IGMM, Montpellier, France) for instructive discussions. The authors want to thank the following researchers for providing essential reagents: C. Dehay (Institute of Brain and Stem Cell Research, INSERM, Bron, France) for proving us with rhesus sperm samples, M. Gorovsky (University of Rochester, Rochester, NY, USA) for his generous gift of the polyG and polyE antibodies, and Y. Ishimi (Mitsubishi-Kasei Institute of Life Sciences, Tokyo, Japan) for kindly providing mAb 4A8. The monoclonal antibody 12G10 developed by J. Frankel and M. Nelson was obtained from the Developmental Studies Hybridoma Bank developed under the auspices of the NICHD and maintained by the University of Iowa.

Received: July 7, 2008
Revised: March 16, 2009
Accepted: May 11, 2009
Published: June 11, 2009

REFERENCES

Bell, P.B., Jr., and Safiejko-Mroczka, B. (1995). Improved methods for preserving macromolecular structures and visualizing them by fluorescence and scanning electron microscopy. Scanning Microsc. *9*, 843–857.

Bré, M.H., Redeker, V., Quibell, M., Darmanaden-Delorme, J., Bressac, C., Cosson, J., Huitorel, P., Schmitter, J.M., Rossier, J., Johnson, T., et al. (1996). Axonemal tubulin polyglycylation probed with two monoclonal antibodies: widespread evolutionary distribution, appearance during spermatozoan maturation and possible function in motility. J. Cell Sci. *109*, 727–738.

Bré, M.H., Redeker, V., Vinh, J., Rossier, J., and Levilliers, N. (1998). Tubulin polyglycylation: differential posttranslational modification of dynamic cytoplasmic and stable axonemal microtubules in Paramecium. Mol. Biol. Cell *9*, 2655–2665.

Bressac, C., Bré, M.H., Darmanaden-Delorme, J., Laurent, M., Levilliers, N., and Fleury, A. (1995). A massive new posttranslational modification occurs on axonemal tubulin at the final step of spermatogenesis in Drosophila. Eur. J. Cell Biol. *67*, 346–355.

Brown, J.M., Marsala, C., Kosoy, R., and Gaertig, J. (1999). Kinesin-II is preferentially targeted to assembling cilia and is required for ciliogenesis and normal cytokinesis in Tetrahymena. Mol. Biol. Cell *10*, 3081–3096.

Chu, D.T., and Klymkowsky, M.W. (1989). The appearance of acetylated alpha-tubulin during early development and cellular differentiation in Xenopus. Dev. Biol. *136*, 104–117.

Dietzl, G., Chen, D., Schnorrer, F., Su, K.C., Barinova, Y., Fellner, M., Gasser, B., Kinsey, K., Oppel, S., Scheiblauer, S., et al. (2007). A genome-wide transgenic RNAi library for conditional gene inactivation in Drosophila. Nature *448*, 151–156.

Dossou, S.J.Y., Bré, M.-H., and Hallworth, R. (2007). Mammalian cilia function is independent of the polymeric state of tubulin glycylation. Cell Motil. Cytoskeleton *64*, 847–855.

Duan, J., and Gorovsky, M.A. (2002). Both carboxy-terminal tails of alpha- and beta-tubulin are essential, but either one will suffice. Curr. Biol. *12*, 313–316.

Eddé, B., de Néchaud, B., Denoulet, P., and Gros, F. (1987). Control of isotubulin expression during neuronal differentiation of mouse neuroblastoma and teratocarcinoma cell lines. Dev. Biol. *123*, 549–558.

Eddé, B., Rossier, J., Le Caer, J.P., Desbruyères, E., Gros, F., and Denoulet, P. (1990). Posttranslational glutamylation of alpha-tubulin. Science *247*, 83–85.

Ersfeld, K., Wehland, J., Plessmann, U., Dodemont, H., Gerke, V., and Weber, K. (1993). Characterization of the tubulin-tyrosine ligase. J. Cell Biol. *120*, 725–732.

Fabrizio, J.J., Hime, G., Lemmon, S.K., and Bazinet, C. (1998). Genetic dissection of sperm individualization in Drosophila melanogaster. Development *125*, 1833–1843.

Fujii-Nakata, T., Ishimi, Y., Okuda, A., and Kikuchi, A. (1992). Functional analysis of nucleosome assembly protein, NAP-1. The negatively charged COOH-terminal region is not necessary for the intrinsic assembly activity. J. Biol. Chem. *267*, 20980–20986.

Ikegami, K., Horigome, D., Mukai, M., Livnat, I., MacGregor, G.R., and Setou, M. (2008). TTLL10 is a protein polyglycylase that can modify nucleosome assembly protein 1. FEBS Lett. *582*, 1129–1134.

Ishimi, Y., Sato, W., Kojima, M., Sugasawa, K., Hanaoka, F., and Yamada, M. (1985). Rapid purification of nucleosome assembly protein (NAP-I) and production of monoclonal antibodies against it. Cell Struct. Funct. *10*, 373–382.

Janke, C., Rogowski, K., Wloga, D., Regnard, C., Kajava, A.V., Strub, J.-M., Temurak, N., van Dijk, J., Boucher, D., Van Dorsselaer, A., et al. (2005). Tubulin polyglutamylase enzymes are members of the TTL domain protein family. Science *308*, 1758–1762.

Kann, M.L., Prigent, Y., Levilliers, N., Bré, M.H., and Fouquet, J.P. (1998). Expression of glycylated tubulin during the differentiation of spermatozoa in mammals. Cell Motil. Cytoskeleton *41*, 341–352.

Lalle, M., Salzano, A.M., Crescenzi, M., and Pozio, E. (2006). The Giardia duodenalis 14–3-3 protein is post-translationally modified by phosphorylation and polyglycylation of the C-terminal tail. J. Biol. Chem. *281*, 5137–5148.

Levilliers, N., Fleury, A., and Hill, A.M. (1995). Monoclonal and polyclonal antibodies detect a new type of post-translational modification of axonemal tubulin. J. Cell Sci. *108*, 3013–3028.

Mans, D.A., Voest, E.E., and Giles, R.H. (2008). All along the watchtower: is the cilium a tumor suppressor organelle? Biochim. Biophys. Acta *1786*, 114–125.

Michaud, E.J., and Yoder, B.K. (2006). The primary cilium in cell signaling and cancer. Cancer Res. *66*, 6463–6467.

Nogales, E. (2000). Structural insights into microtubule function. Annu. Rev. Biochem. *69*, 277–302.

Redeker, V., Levilliers, N., Schmitter, J.M., Le Caer, J.P., Rossier, J., Adoutte, A., and Bré, M.H. (1994). Polyglycylation of tubulin: a posttranslational modification in axonemal microtubules. Science *266*, 1688–1691.

Redeker, V., Levilliers, N., Vinolo, E., Rossier, J., Jaillard, D., Burnette, D., Gaertig, J., and Bré, M.H. (2005). Mutations of tubulin glycylation sites reveal cross-talk between the C termini of alpha- and beta-tubulin and affect the ciliary matrix in Tetrahymena. J. Biol. Chem. *280*, 596–606.

Regnard, C., Desbruyères, E., Denoulet, P., and Eddé, B. (1999). Tubulin polyglutamylase: isozymic variants and regulation during the cell cycle in HeLa cells. J. Cell Sci. *112*, 4281–4289.

Regnard, C., Desbruyères, E., Huet, J.C., Beauvallet, C., Pernollet, J.C., and Eddé, B. (2000). Polyglutamylation of nucleosome assembly proteins. J. Biol. Chem. *275*, 15969–15976.

Schneider, A., Plessmann, U., and Weber, K. (1997). Subpellicular and flagellar microtubules of Trypanosoma brucei are extensively glutamylated. J. Cell Sci. *110*, 431–437.

Sjöblom, T., Jones, S., Wood, L.D., Parsons, D.W., Lin, J., Barber, T.D., Mandelker, D., Leary, R.J., Ptak, J., Silliman, N., et al. (2006). The consensus coding sequences of human breast and colorectal cancers. Science *314*, 268–274.

Thazhath, R., Liu, C., and Gaertig, J. (2002). Polyglycylation domain of beta-tubulin maintains axonemal architecture and affects cytokinesis in Tetrahymena. Nat. Cell Biol. *4*, 256–259.

van Dijk, J., Rogowski, K., Miro, J., Lacroix, B., Eddé, B., and Janke, C. (2007). A targeted multienzyme mechanism for selective microtubule polyglutamylation. Mol. Cell *26*, 437–448.

van Dijk, J., Miro, J., Strub, J.-M., Lacroix, B., Van Dorsselaer, A., Eddé, B., and Janke, C. (2008). Polyglutamylation is a post-translational modification with a broad range of substrates. J. Biol. Chem. *283*, 3915–3922.

Vinh, J., Langridge, J.I., Bré, M.H., Levilliers, N., Redeker, V., Loyaux, D., and Rossier, J. (1999). Structural characterization by tandem mass spectrometry of the posttranslational polyglycylation of tubulin. Biochemistry *38*, 3133–3139.

Wloga, D., Rogowski, K., Sharma, N., Van Dijk, J., Janke, C., Eddé, B., Bré, M.H., Levilliers, N., Redeker, V., Duan, J., et al. (2008). Glutamylation on alpha-tubulin is not essential but affects the assembly and functions of a subset of microtubules in Tetrahymena thermophila. Eukaryot. Cell *7*, 1362–1372.

Wloga, D., Webster, D., Rogowski, K., Bré, M.-H., Levilliers, N., Jerka-Dziadosz, M., Janke, C., Dougan, S.T., and Gaertig, J. (2009). TTLL3 protein generates tubulin glycylation and regulates ciliogenesis. Dev. Cell. Published online June 15, 2009. 10.1016/j.devcel.2009.04.008.

Xia, L., Hai, B., Gao, Y., Burnette, D., Thazhath, R., Duan, J., Bré, M.H., Levilliers, N., Gorovsky, M.A., and Gaertig, J. (2000). Polyglycylation of tubulin is essential and affects cell motility and division in Tetrahymena thermophila. J. Cell Biol. *149*, 1097–1106.

Xie, R., Clark, K.M., and Gorovsky, M.A. (2007). Endoplasmic reticulum retention signal-dependent glycylation of the hsp70/grp170-related pgp1p in tetrahymena. Eukaryot. Cell *6*, 388–397.